Automatic Ultrasonic Thermometry[1]

X.B. Mi [2], S.Y. Zhang [2,4], J.J Zhang [2,3] and Y.T. Yang [2]

[1] Paper presented at the Fifteenth Symposium on Thermophysical Properties, June 22-27, 2003, Boulder, Colorado, U.S.A.

[2] Lab of Modern Acoustics, Institute of Acoustics, Nanjing University, Nanjing, 210093, China

[3] Department of Electronic Engineering, University of Science and Technology of China, Hefei, 230026, China

[4] To whom correspondence should be addressed. E-mail: paslab@nju.edu.cn

ABSTRACT

Based on the principle that the velocity of sound in any material is a function of temperature, over the past several decades, ultrasonic thermometries have been evolving as a new temperature measurement technology. However, most of the ultrasonic thermometries so far as now are with lower automatization, lower accuracy and difficult in realizing on-line control. A thermometer, which automatically measures temperature by using an ultrasonic pulse-echo technique and zero point-around method, is described in this paper. The experimental and theoretical results demonstrate that this thermometer is capable for automatically and durably measuring temperature with a time resolution of 0.2 us.

KEY WORDS: on-line control; temperature measurement; thermometry; ultrasound.

1. INTRODUCTION

In many industrial processes, such as refining, roasting etc., the online control of temperature is often very important as far as to saving energy, guaranteeing product's quality and raising the productivity etc. Up to now, thermocouples and radiation thermometers are two main methods for measuring temperature in industry. Accurate and sensitive as the thermocouple is, it can not work durably in high temperature and is hard to realize on-line control. With the development of pthotoelectronic techniques, great improvements have been made in radiation thermometer. While, because of its susceptibility to fume and mist, accurate measurement is difficult to be obtained in the above hostile environments.

Over the past several decades, ultrasonic thermometry has been evolving as a new temperature measurement technology for environments where thermocouples, radiation pyrometers and other conventional instruments have failed to operate satisfactorily. Its principle is that the velocity of sound in any object is a function of temperature, such as, in idea gas the velocity is direct proportional to the square root of the absolute temperature, in most of the liquids the dependency is linear, and in solid objects the velocity generally decreases with the increment of the temperature. Thus, if the velocity

of the sound is measured, the temperature is measured. Generally, ultrasonic thermometries can be divided into two main types, pulse-echo technique or resonance method. Each has advantages or disadvantages [1].

The evolution of the ultrasonic thermometry is reflected through numerous papers published and a series of applications in industry achieved [2-5]. However, most of the thermometries above are with lower automatization, lower accuracy and difficult in realizing on-line control. A thermometer, which automatically measures temperature by using a pulse-echo technique and zero point-around (ZPA) method, is described in this paper. Since the time resolution is 0.2 us, a better sensitivity and accuracy of temperature measurement can be achieved. The experimental measurements and theoretical analyses are also performed to verify the measurement correctness of the thermometer.

2. PRINCIPLE OF AUTOMATIC TEMPERATURE MEASUREMENT

When a longitudinal sound wave is excited at one end of a cylindrical sample, the direct wave and echo waves can be received by a receiver at the other end. In the ZPA method the zero-crossing points (point A and point B in Fig. 1) of the wave are chosen as the measurable time. The time interval between points A and B is

$$t_{BA} = t_B - t_A \tag{1}$$

where t_A and t_B are the travel time of points A and B respectively. In normal practice, the averaging method is adopted in order to improve the accuracy and signal-to-noise ratio. When the temperature of the sample changes, the zero crossing points move as a result

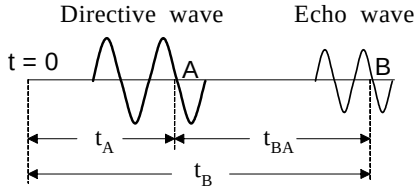

Fig. 1. Wave signals at the receiver

of the change of the sound velocity. Therefore, how to correctly trace the zero-crossing point is the key to realizing automatic measurement. As shows in Fig. 2, we divide the travel time of t into two parts, t_1 and t_2. When the zero-crossing points move, t_1 and t_2 change consequently. Whereas t_1 can always be maintained a time interval of t_2 to the selected zero-crossing point (point A in Fig. 2) by the following equation's iterating

$$\begin{cases} t_1^{(i)} = t_1^{(i-1)} + t_2^{(i-1)} - t_{\max} & t_2^{(i-1)} > t_{\max} \\ t_1^{(i)} = t_1^{(i-1)} + t_2^{(i-1)} + t_{\min} & t_2^{(i-1)} < t_{\min} \\ t_1^{(i)} = t_1^{(\text{i-1})} & t_{\min} \le t_2^{(i-1)} \le t_{\max} \end{cases} \tag{2}$$

where t_{min} and t_{max} are two constants and i=1,2,etc. When propagating distance is determined, the measurement of the sound velocity is equivalent to that of the travel

time. Since the velocity is a function of temperature, automatic temperature measurement thus can be achieved by simply measuring the travel time.

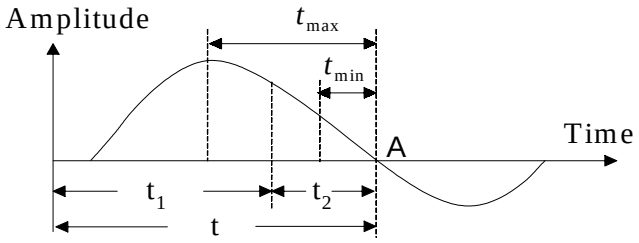

Fig. 2. Principle of automatic temperature measurement

3. SETUP OF ULTRASONIC THERMOMETER

Fig. 3(a) shows the functional diagram of the thermometer, which mainly consists of a graphite bar, a PZT, a circuit board and a computer. The central frequency of the generated ultrasound is about 11 KHZ. The proper length of the graphite bar is important, because if the length is either too long or too short the precision and resolution of the measurement will be reduced. The graphite bar was heat-treated at nearly 3273 K, thus has a better capacity of heat conduction and oxidation resistance even in high temperature. Since the thermal expansion coefficient of the graphite is very small (less than 2.75×10^{-6}/K in the temperature range of 293 K to 1273 K), the length variation caused by the thermal expansion is neglected here.

Fig.3 (b) shows the schematic diagram of the operation process of the thermometer. The computer generates digital pulse signals of a certain frequency at a regular time interval. Through a sampling board, a trigger circuit, a power amplifier and a ptotoisolator, the generated electrical pulses with short duration and enough power exert to the PZT. The PZT converts these electrical pulses into ultrasonic pulses, which travel down the graphite bar. Then the reflections travel back to the PZT and are converted back to electrical pulses. The signals, which are generally very small, before inputting into the ptotoisolator, must be amplified big enough to least the nonlinear distortion. Next, after the frequency selective circuit and the digital sampling board, these signals are inputted to the computer to display and at the same time the signals are transformed into square waves through the shaping unit. According to the sampling figure, one zero-crossing point will be chosen and the $t_1^{(0)}$ will be recorded. At the time of $t_1^{(0)}$, the time counter is driven to time till the rising edge of the square wave and the time interval in the counter is just the $t_2^{(0)}$. If t_2 is between t_{min} and t_{max}, the zero crossing is valid and $t = t_1 + t_2$ is computed and saved. Therefore the automatic temperature measurement is accomplished.

The cycle of the counter is 0.1 us, then a time accuracy better than 0.2 us can be obtained after averaging the multiple measurements. Since the industrial conditions are usually very complicated, hostile, with bigger noise and potential unsafe factors, before inputting into the computer, the signals are isolated through the photoisolator, which can reduce the noise as well as protect the computer.

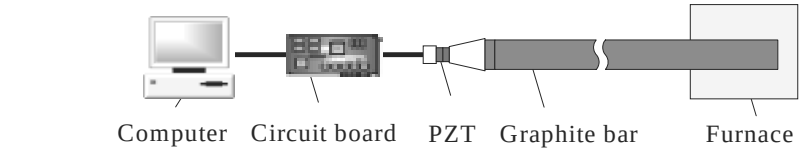

(a)

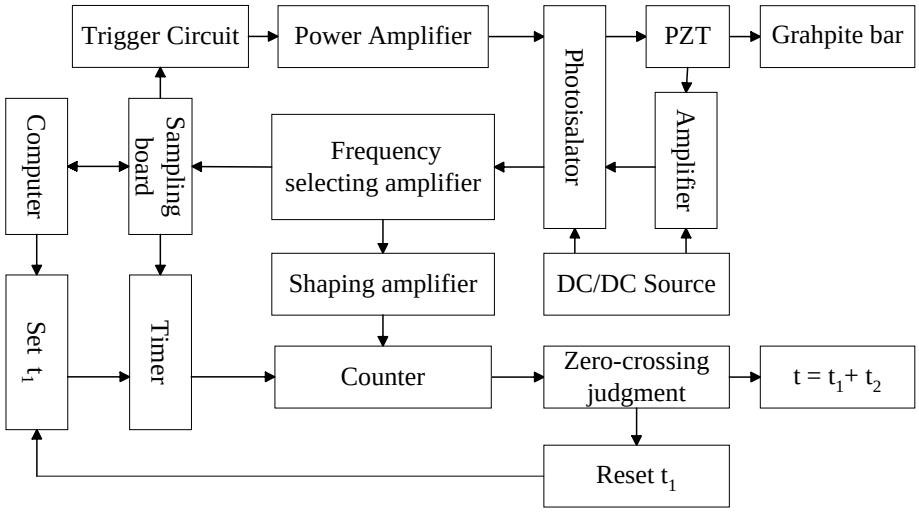

(b)

Fig. 3. Schematic diagram of the ultrasonic thermometer

4. TEMPERATURE MEASUREMENT EXPERIMENT

The experimental setup is shown in Fig. 3 (a), where one end of the graphite bar is putted into an electrically heated furnace, which has a chamber with 0.28 meters long. The temperature of the center part of the chamber can be automatically displayed and controlled. Since the length of the graphite bar inside the furnace is about 0.28 meters, the temperature distribution along the graphite bar is not uniform. The rising time of the first echo is measured as the travel time of the ultrasound. The variation of the travel time is also calculated. Then the ultrasound velocity C can be obtained through the following equation

$$C = \frac{2LC_0}{2L + C_0\Delta t} \tag{3}$$

where L is the length of the graphite bar, C_0 is the velocity at room temperature and Δt is the variation of the travel time. The data above are listed in Tab. I.

We can see from Tab. I that the variation of the travel time reaches a bigger value of 14.2 us at 703 K, then decreases with the temperature rising, decreasing 2 us at 878 K. Consequently, the ultrasound velocity attains a minor value of 1905 (m/s) at 703 K and increases with the temperature rising thereafter. During the experiments, the system keeps track of the ultrasound travel time accurately and runs stably with the time resolution of 0.2 us even after continuously working more than 48 hour. The capacity of tracking allows a time variation within 25 us.

Table I. Travel time and velocity

Temperature (K)	Travel time (us)	Variation of travel time (us)		Average velocity (m/s)	
		Experiment	Theory	Experiment	Theory
Room temperature	1560.2	0	\	1923	1906
463	1566.8	6.6	5.36	1914	1900
523	1568.6	8.4	7.26	1912	1897
583	1570.8	10.6	9.40	1910	1894
703	1574.4	14.2	11.85	1905	1891
878	1572.4	12.2	10.29	1908	1893

5. THEORETICAL ANALYSIS

5.1. Temperature distribution

The temperature analysis model is shown in Fig. 4, in which one end of the graphite bar ($0 \le z \le z_0$) lying in the furnace is heated with a uniform heat flux of q. The other part ($z_0 < z \le L$) is exposed in the air with temperature T_0, and heat is lost to the surroundings by radiation and convection. The model can be expressed by the thermal conduction equation and boundary conditions

$$\frac{\partial}{\partial r}(k_r \frac{\partial T}{\partial r}) + \frac{k_r}{r}\frac{\partial T}{\partial r} + \frac{\partial}{\partial z}(k_z \frac{\partial T}{\partial z}) = 0 \tag{4}$$

$$k_r \frac{\partial T}{\partial r} n_r + k_z \frac{\partial T}{\partial z} n_z = q \qquad (0 \le z \le z_0) \tag{5}$$

$$k_r \frac{\partial T}{\partial r} n_r + k_z \frac{\partial T}{\partial z} n_z = (h + h_r)(T_0 - T_s) \qquad (z_0 < z \le L) \tag{6}$$

$$h_r = \eta f \sigma (T_s^{\,2} + T_0^{\,2})(T_s + T_0) \tag{7}$$

where k_r and k_z are the radial and axial heat conductivities respectively, n_r and n_z are the radial and axial cosine vectors respectively, h is the convection coefficient, h_r is the equivalent convection coefficient of the radiation, T_s is the surface temperature of the graphite bar, η is the emissivity of the radiating surface, f is the shape factor and σ is the Boltzmann constant. Because of the non-linearity of the thermal conduction equation, it is generally impossible to find an analytical solution. The calculations presented here are based on the Finite-Element-Method (FEM).

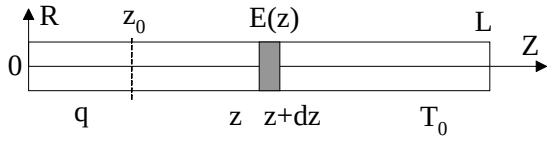

Fig. 4. Temperature analysis model of the graphite bar

First, an approximate function $\overline{T}$ is assumed and substituted into the equations of (4)-(7). Residuals are generated for its approximation. According to the Weighted Residual Method (WRM) and by the parts integration method and the Green's theorem, one can obtain

$$-\int_{\Omega}\left[\frac{\partial\omega_1}{\partial r}\left(k_r\frac{\partial\overline{T}}{\partial r}\right)+\frac{\partial\omega_1}{\partial z}\left(k_z\frac{\partial\overline{T}}{\partial z}\right)\right]d\Omega+\oint_{\Gamma}\omega_1\left(k_r\frac{\partial\overline{T}}{\partial r}n_r+k_z\frac{\partial\overline{T}}{\partial z}n_z\right)d\Gamma+\int_{\Omega}\frac{\omega_1 k_r}{r}\frac{\partial\overline{T}}{\partial r}d\Omega$$

$$+\int_{\Gamma_2}\omega_3\left(k_r\frac{\partial\overline{T}}{\partial r}n_r+k_z\frac{\partial\overline{T}}{\partial z}n_z-(h+h_r)(T_0-\overline{T}_s)\right)d\Gamma+\int_{\Gamma_1}\omega_2\left(k_r\frac{\partial\overline{T}}{\partial r}n_r+k_z\frac{\partial\overline{T}}{\partial z}n_z-q\right)d\Gamma=0 \quad (8)$$

where $\omega_i, i=1,2,3$ denote the weighted functions and $\Gamma=\Gamma_1+\Gamma_2$.

Then the object is meshed into finite elements and the temperature of any point within the elements is interpolated by the temperatures of the nodes, that is

$$T=\sum_{i=1}^{n_e}N_i(r,z)T_i \quad =NT^e \quad (9)$$

where T_i denotes the temperature of the node, $N_i(r,z)$ is the linear interpolation function and $N=[N_1\ N_2\cdots N_{n_e}]$, where n_e is the number of the node of each element. According to the Galerkin method, choose the weighted function $\omega_1=N_j$ and $\omega_2=\omega_3=-N_j$ on the boundaries, where $j=1,2\cdots n$ and n denotes the total number of the nodes of the whole meshed graphite bar. Substitute the above equation into the equations (8) and change it to the general FEM form:

$$KT=P \quad (10)$$

where *K* is the $n\times n$ matrix of heat conduction, $T=\left[T_1T_2T_3\cdots T_n\right]'$ is the $n\times1$ matrix of the temperatures of the nodes, *P* is the $n\times1$ matrix of the temperature loadings. Matrix *K* and *P* can be expressed by

$$K_{ij}=\sum_e\int_{\Omega^e}(k_r\frac{\partial N_i}{\partial r}\frac{\partial N_j}{\partial r}+k_z\frac{\partial N_i}{\partial z}\frac{\partial N_j}{\partial z}-N_i\frac{k_r}{\bar{r}}\frac{\partial N_j}{\partial z})d\Omega+\sum_e\int_{\Gamma_2^e}N_i(h+h_r)N_j d\Gamma \quad (11)$$

$$P_i=\sum_e\int_{\Gamma_1^e}N_i q d\Gamma+\sum_e\int_{\Gamma_2^e}hN_iT_0 d\Gamma+\sum_e\int_{\Gamma_2^e}h_rN_iT_0 d\Gamma \quad (12)$$

where $i,j=1,2,\cdots,n$ and $\bar{r}$ denotes the central point of each element.

By solving equation (10), one can obtain the temperatures of n nodes. When the bar is meshed small enough, the accurate solution can be obtained. The numerical results are shown in Fig. 5.

5.2. Calculation of the travel time and ultrasonic velocity

Fig. 6 shows the dependence of the Young's modulus on temperature for graphite

heat-treated at 3273 K [6], from which we can see that the Young's modulus is not the monotonic function of temperature, a minimum appearing about 573 K. Based on the sound velocity equation $C = \sqrt{E/\rho}$, the travel time of the reflective ultrasound can be expressed by

$$t_1 = \int_0^L \frac{2\sqrt{\rho}}{\sqrt{E(z)}} dz \tag{13}$$

where E is modulus, ρ is density. So the variation of the travel time is

$$\Delta t = 2\sqrt{\rho}\left(\int_0^L \frac{1}{\sqrt{E(z)}} dz - \frac{L}{\sqrt{E_0}} \right) \tag{14}$$

where $\Delta t = t_1 - t_0$, t_0 is the whole travel time at room temperature, E_0 is the modulus at room temperature. The numerical calculation can be obtained by trapezoid formula

$$\Delta t = 2\sqrt{\rho} \cdot \left\{ \sum_{j=0}^{Q-1} \frac{h}{2} \left[\frac{1}{\sqrt{E(z_j)}} + \frac{1}{\sqrt{E(z_{j+1})}} \right] - \frac{L}{\sqrt{E_0}} \right\} \tag{15}$$

where Q is the dividing number of L, $h = L/Q$ and $E(z_j)$ can be derived by substituting the z_j into the least-square-fitting equation of the data shown in Fig. 6. Herein, Q is chosen 150 and h is 0.01 m. The truncation error from this calculation is less than 6.4×10^{-5} and the standard error of the fitting is less than 2.5×10^{-3}.

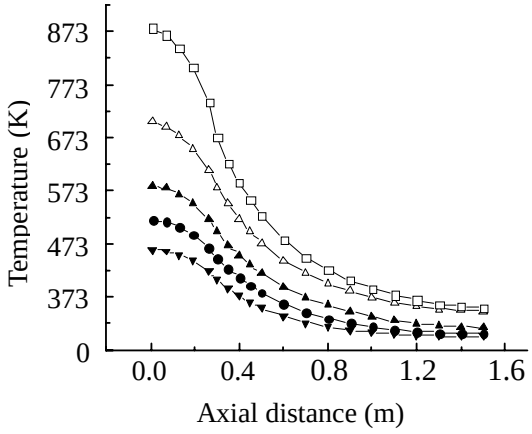

Fig. 5. Axial temperature distribution of the graphite bar at different temperatures

Then, the theoretical ultrasonic velocity can be obtained by equation (3) and the velocity at room temperature is 1906 (m/s), which is calculated by the equation $C = \sqrt{E_0/\rho}$. The theoretical ultrasonic travel times and velocities at different temperatures are also listed in Tab. I.

From Tab. I, we can see that the theoretical values are in good agreement with the

experimental results. The experimental data of ultrasonic travel time and velocity do not vary monotonically, resulting from the non-monotonic dependence of the Young's modulus on temperature, and the experimental data verify it inversely. Further, because the temperature distribution of the graphite bar is not uniform, the Young's modulus values may lie in the two sides of the minimum. As a result, the experimental data of the variation of the ultrasonic travel time or velocity are very small. In fact, the theoretical variation of the travel time is up to 18 us in the graphite bar from the room temperature to 573 K. It is up to 81 us while temperature changes from 573 K to 1273 K. Therefore, by the thermometer with a 0.2 us time resolution, a better measurement sensitivity of 3.2 K or 1.7 K can be obtained in the temperature range of 293 K to 573 K or in the range of 573 K to 1273 K, respectively.

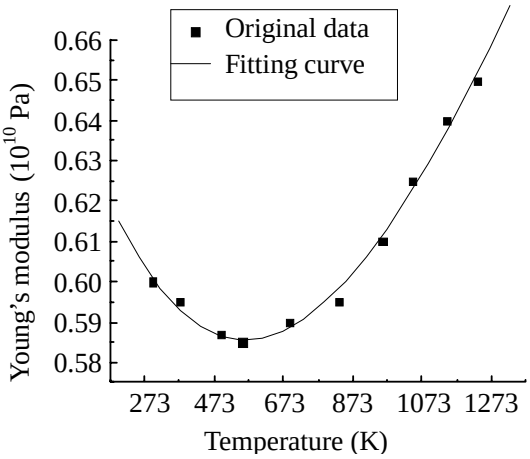

Fig. 6. Dependence of the Young's modulus on temperature for graphite heat-treated at 3273 K [6]

6. DISCUSSION AND CONCLUSION

A thermometer, which can automatically measure temperature by using an ultrasonic pulse-echo technique and zero point-around method, is described in this paper. The experimental and theoretical results demonstrate that this thermometer is capable for automatically and durably measuring temperature with a 0.2 us time resolution. The non-monotonic dependence of the Young's modulus on temperature makes the variation of the ultrasonic travel time and velocity do not vary monotonically.

The thermometer is capable of on-line control in a wide range of temperature with a better sensitivity and accuracy.

However, when it operates in high temperature, the PZT must be cooled very well or the $LINBO_3$ with a higher Curie temperature must be substituted, because the PZT can not work properly for long time. Additionally, the resolution of the graphite bar's temperature distribution is also helpful for the thermometer's calibration in high temperature. Since the thermocouple generally can not measure the temperature above 2273 K, However, on that condition we can still obtain the temperature and calibrate the measurement through measuring the low temperatures of the other end and further

figuring the high temperature according to the temperature distribution curves.

REFERENCES

1. C.Z. Sun, *J. Ast. Metr. Mea.(China)* **4**: 35(1995).
2. L.C. Lynnworth, E.H. Carnevale, in *Temperature: Its Measurement and Control in Science and Industry*, Vol. 4 (ISA, Pittsburgh, 1972), pp. 715-732.
3. H.A.Tasman, M. Campana, et al, in *Temperature: its Measurement and Control in Science and Industry*, Vol. 5, (AIP, New York, 1982), pp.1191-1196.
4. Y.C. Li, P.D. Sun, *Proceedings Of The China-Japan Joint Conference On Ultrasonics*, (OC, Nanjing, 1987), pp. 239-242.
5. S.C. Wilkins, in *Temperature: Its Measurement and Control in Science and Industry*, Vol. 6, (AIP, New York, 1992), pp. 1027-1032.
6. I.B. Mason, R.H. Knibbs, *Carbon* **5**:493(1967).